PERGAMON

Journal of Atmospheric and Solar-Terrestrial Physics 63 (2001) 473–479

Journal of ATMOSPHERIC AND SOLAR-TERRESTRIAL PHYSICS

www.elsevier.nl/locate/jastp

11366

The geotail and ring current dynamics under disturbed conditions

V.V. Kalegaev[a,*], I.I. Alexeev[a], Ya.I. Feldstein[b]

[a] *Institute of Nuclear Physics, Moscow State University, Moscow 119899, Russia*
[b] *IZMIRAN, 142092 Troitsk, Moscow region, Russia*

Received 8 November 1999; accepted 27 April 2000

Abstract

Complex study of satellite and ground-based data as well as theoretical modelling has been carried out to estimate the roles of different magnetospheric sources of geomagnetic disturbances. The geotail and ring current dynamics during the magnetic storm on 23–27 November 1986 were calculated using the dynamic paraboloid model of the magnetospheric magnetic field. The solar wind data and magnetospheric indices were used to calculate the time-dependent paraboloid model parameters. The auroral oval boundaries were determined using the DMSP electron fluxes precipitation data. The ring current magnetic field was calculated using data from AMPTE/CCE measurements of the ring current energetic ion fluxes. The comparison of the model calculations with Dst and GOES-6 satellite data was carried out. It was found that magnetopause currents', ring current's and tail current's contributions to Dst are of about the same order of magnitude in the course of the magnetic storm on 23–27 November 1986. The energy stored in the tail correlates strongly with the power delivered from the solar wind to the magnetosphere. The total energy of the ring current particles increases when the interplanetary magnetic field is southward. Ring current growth stops during periods of high auroral activity.

Keywords: Magnetosphere; Magnetic storm; Magnetospheric tail; Ring current

1. Introduction

The large-scale magnetospheric magnetic field sources are highly time dependent and may undergo rapid changes during magnetic storms. Their variations have a different time scale and determine the complex structure of the magnetospheric magnetic field. The hourly averaged Dst profile shows the clear influence of the ring current, Chapman–Ferraro currents and magnetospheric tail currents. All these magnetospheric magnetic field sources give a significant contribution to Dst in the course of magnetic disturbances (see Campbell, 1973; Alexeev et al., 1992, 1996; Arykov and Maltsev, 1993; Dremukhina et al., 1999). As has been noted in Alexeev et al. (1996) the contribution of tail currents can be compared to the Dst value.

The magnetospheric tail current consists of two parts: dawn–dusk currents across the magnetospheric tail and closure currents on the magnetopause. The tail current magnetic field lines are inside the tube which is formed by these current loops. In the distant northern tail lobe the magnetic field vector is earthward but in the southern one it has the opposite direction. The tail current loops are approximately orthogonal to the equatorial plane in the distant tail. In the inner magnetosphere the tail current magnetic field lines cross the equatorial plane. The tail current loops bend over the equatorial plane: the closer the crosstail currents are to the inner edge of the tail current sheet, the more equatorial closure currents there are on the dayside magnetopause.

During quiet times, the contribution of the tail currents to the horizontal component of the magnetic field on the Earth's surface is ~15–20 nT. However, in the course of a substorm, a significant enhancement of the tail current system's magnetic field is often observed (Kaufmann, 1987; Kokubun et al., 1996; Ho and Tsurutani, 1997). The main

* Corresponding author. Tel.: +7-095-939-1915; fax: +7-095-939-3553.

E-mail address: klg@dec1.npi.msu.su (V.V. Kalegaev).

1364-6826/01/$ - see front matter
PII: S1364-6826(00)00162-0

source of these disturbances is the intense radially localized currents in the earthward edge of the tail current sheet, which appear during substorm activations (see Pulkkinen et al., 1992). These currents, closing over the dayside magnetopause, form loops which are located near the equatorial plane. The magnetic field of these loops in the internal magnetosphere is similar to the ring current field. During periods of strong disturbances, when the inner edge of the current sheet moves earthward and the magnetopause stand-off distance decreases, these currents may cause a rather intense disturbance of the magnetic field at the Earth's surface comparable with a ring current-related disturbance. Although these currents exist on substorm-related time scales and may rise and fall during 1 h, they determine the general level of tail current activity in the course of more slow processes such as a magnetic storm. For the magnetic storm on 23–24 March 1969 the tail current contribution into Dst was found to be about 150 nT during periods of substorm activations (in accordance with calculations in Alexeev et al., 1996). In the paper by Turner et al. (2000) the tail current contribution into Dst during event on 10–12 January 1997 was estimated to be about of 25% of Dst. However the tail current-closure currents as well as the tail current-inner edge dynamics were not taken into account, so the tail current magnetic field was apparently underestimated.

More exact results about the magnetospheric magnetic field dynamics can be obtained on substorm-related time scales. The substorm dipolarisation is responsible for efficient earthward transport of plasma sheet particles deep in the inner magnetosphere, so the ring current energy rises during substorm expansion phase (Fok et al., 1999). The substorm current wedge formation after substorm onset produces positive magnetic field-horizontal component disturbance on the Earth's surface. The study of the longitudinal distribution of the magnetospheric magnetic field variations on the Earth's surface showed a significant contribution from the substorm current wedge to Dst during the substorm expansion phase (Friedrich et al., 1999). When the substorm activity diminishes the tail current contribution into Dst becomes smaller. It was suggested by Iyemory and Rao (1996) that decay of the magnetospheric tail current after substorm onset is responsible for the decay of the Dst index. In general, the geotail dynamics on substorm-related time scales is much more complex process than the stormtime geotail dynamics. Some questions about the magnetospheric dynamics during substorms as well as about the role of substorms in developing stormtime ring current will be considered below.

The contribution of various magnetospheric sources of magnetic field to the magnetic field variations observed at the Earth's surface in the course of the magnetic storm on 23–27 November 1986 will be considered in this paper. We will investigate the questions about the Dst sources, as well as about the magnetospheric energy dynamics during magnetospheric disturbances. We will use the approach firstly proposed by Alexeev et al. (1992, 1996) however the ring current contribution to Dst will be obtained by independent data from the AMPTE/CCE satellite, using methods of calculations described in detail by Greenspan and Hamilton (2000). The dynamic paraboloid model of magnetic field will be used to estimate the magnetic field of magnetospheric sources during magnetic storm. Unlike Alexeev et al. (1996) and Dremukhina et al. (1999) some new methods will be used to calculate the model input parameters (the magnetopause stand-off distance and the tail lobe magnetic flux). Moreover, correlation between the solar wind energy input rate into the magnetosphere and tail-stored energy as well as the dynamics of ring current energy on substorm-related time scales will be considered.

2. Calculations

In calculations, a paraboloid model of the Earth's magnetosphere was used (Alexeev, 1978; Alexeev et al., 1996), enabling the description of the dynamics of various components of the magnetospheric magnetic field. The magnetic field in the magnetosphere is created by the following sources: (1) the geomagnetic dipole; (2) the ring current; (3) the magnetotail current system including the dawn–dusk current across the tail current sheet and the closure currents on the magnetopause; (4) the currents on the magnetopause screening the dipole field; and (5) the currents on the magnetopause screening the ring current magnetic field. The paraboloid model is dynamical model. The most interesting results were obtained with the paraboloid model when concrete magnetospheric disturbances were studied (Alexeev et al., 1992, 1996; Kalegaev et al., 1998). The paraboloid model enables calculation of each magnetospheric source separately. This fact is significant when studying dynamical processes, since different magnetospheric sources of the magnetic field change with different characteristic times. The paraboloid model input parameters are the following: the geomagnetic dipole tilt angle ψ; the magnetopause stand-off distance R_1; the distance to the inner edge of the tail current sheet R_2; the magnetic flux through the tail lobes Φ_∞; the ring current field at the Earth's centre B_R. Their physical meaning is quite clear, so they can be determined from the available observed data using the so-called submodels. Unlike the empirical models this is an analytical one and has no limitations on the values of data used for calculations. At each moment the input parameters define the instantaneous state of the magnetosphere.

The important feature of the paraboloid model is that magnetospheric magnetic field depends on empirically measured parameters not directly but via input parameters. In different case studies we can use the different submodels for the same input parameters, depending on data available. Some submodels can demand a wide variety of data, and the paraboloid model gives more accurate results with additional data. On the other hand, investigation of the processes when a lot of additional empirical data is available allows one to estimate the model accuracy and applicability.

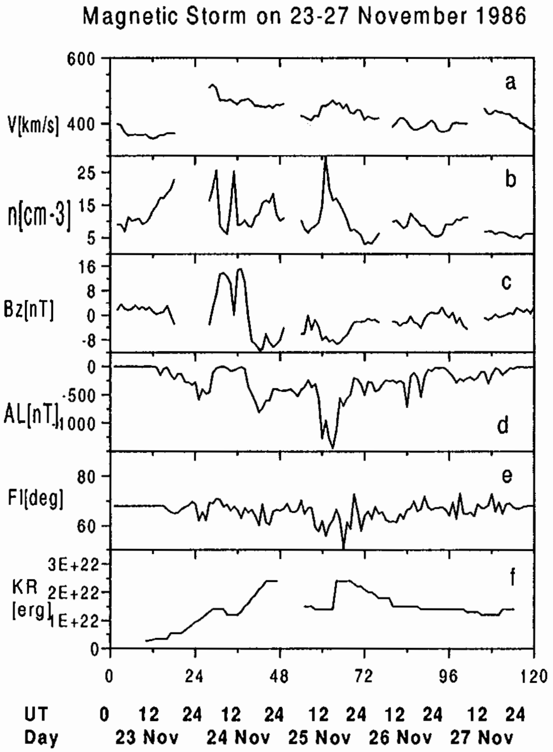

Fig. 1. Empirical data for calculations of the model input parameters: solar wind velocity (km/s) (a), and density (cm^{-3}) (b), IMF B_z component (nT) (c); AL (nT) (d), latitude of the midnight equatorial boundary of the auroral oval φ (degrees) (e), total energy of ring current particles (erg) (f) in the course of the magnetic storm on 23–27 November 1986.

We calculate the magnetospheric magnetic field variations using data obtained in the course of the magnetic storm on 23–27 November 1986. Figs. 1a, b and c present data of the solar wind parameters. These data enable calculation of the geocentric distance R_1 to the subsolar point on the magnetopause as a function of the solar wind dynamical pressure and the interplanetary magnetic field (IMF) B_z component. The modified parabolic magnetopause model by Kalegaev and Lyutov (2000) (valid in the region $X_{GSM} > -20R_E$) which is based on magnetopause crossings data collected by Sibeck et al. (1991) was used:

$$R_1 = \begin{cases} (10.2 + 0.18B_z\ [\text{nT}])(P\ [\text{nPa}]/2.63)^{-1/6} & \text{for } B_z > 0, \\ (10.2 + 0.03B_z\ [\text{nT}])(P\ [\text{nPa}]/2.47)^{-1/6} & \text{for } B_z > 0. \end{cases}$$

The magnetospheric boundary in Kalegaev and Lyutov (2000) is the best fit to the empirical data of magnetopause crossings in the region $X_{GSM} > -20R_E$ and pressure balance at the subsolar point is approximately achieved.

The equatorward boundary of the auroral oval was assumed to be projected along magnetic field lines at the earthward edge of the magnetotail current sheet. The location of the midnight equatorward boundary of the auroral oval φ (see Fig. 1e) was calculated by Kalegaev et al. (1998) from data of high-latitude auroral precipitation measured by the DMSP F6 and F7 satellites. Projection of the equatorial boundary of the oval at midnight along field line of the magnetic dipole enables determination of the distance to the inner edge of the magnetotail current sheet, R_2.

In the paraboloid model of the magnetosphere the tail lobe magnetic flux Φ_∞ does not increase infinitely when moving to the night side from the Earth, although the magnetosphere's diameter increases. In accordance with Alexeev et al. (1996), it will be assumed that the magnetic flux across the tail lobe is a sum of two terms

$$\Phi_\infty = \Phi_0 + \Phi_s. \tag{1}$$

The former term, $\Phi_0 = 370$ MWb, corresponds to a slow adiabatic evolution of the geomagnetic tail. The latter term is associated with the manifestation of substorm activity in the magnetosphere. Based on the results of Lopez and von Rosenvinge (1993), the relation between auroral activity and intensity of the tail magnetic field is chosen in the form (see Alexeev et al., 1992, 1996)

$$\Phi_s = -\pi\ \text{AL}\ (2R_2 + R_1)^{1/2}/14. \tag{2}$$

Unlike Alexeev et al. (1996) when the ring current magnetic field parameters were calculated using characteristics of the Dst profile, the Dessler–Parker–Scopke equation (Dessler and Parker, 1959; Sckopke, 1966)

$$B_R/B_s = -2K_R/3U_m \tag{3}$$

is used now to obtain the magnetic field disturbance produced by the ring current. Here B_R is the magnetic disturbance by the ring current in the Earth's centre, B_s the dipole field at the Earth's equator, K_R is the total energy of ring current ions and U_m is the geodipole magnetic field energy beyond the Earth. Measurements onboard the AMPTE/CCE satellite of the energetic ion fluxes in the region of the ring current enable the estimation of the total energy of ions in the course of the magnetic storm under consideration. The ring current particles' energy was integrated over the L-shell range of 2–7. The method of calculation is described in detail by Greenspan and Hamilton (2000), where DPS equation validity during magnetic storm was investigated. The assumption about the ring current symmetry during magnetic storm was used. Although this assumption is not quite accurate during magnetic storm main phase, it was shown that DPS holds well on average. Fig. 1g shows the total energy of ring current particles K_R in the course of a magnetic storm on 23–27 November 1986.

In Section 3 we will compare model calculations with measurements (from near-equatorial stations (Dst) and from the GOES-6 satellite). Fig. 2 represents the general scheme of Dst calculation. A lot of independent satellite measurements in the solar wind, in the polar ionosphere, and in the ring current region as well as on-ground measurements

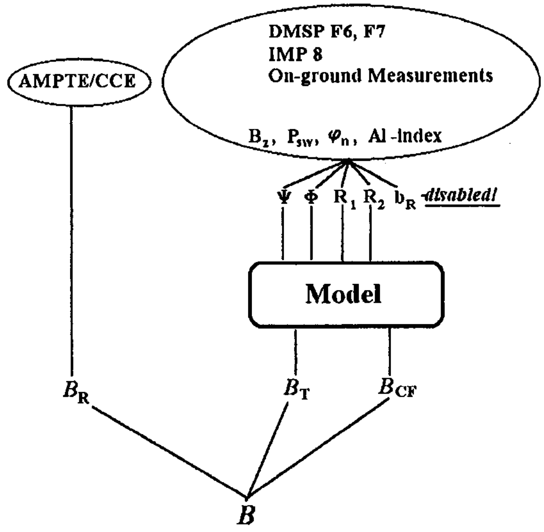

Fig. 2. The general scheme of calculations.

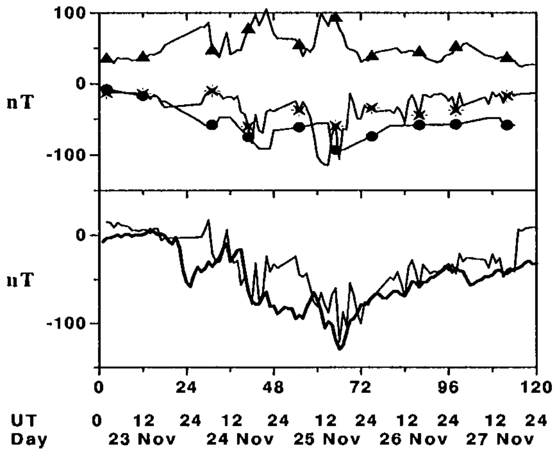

Fig. 3. Magnetic field of currents on the magnetopause (triangles), tail current system (asterisks) and the ring current magnetic field (solid circles) (nT) (a), and Dst (heavy solid line) and total magnetic field, B_M (nT) (b), calculated on the Earth's surface in the course of the magnetic storm on 23–27 November 1986.

were used as input parameters. The Chapman–Ferraro currents and tail current magnetic field variations on the Earth's surface were calculated in terms of the paraboloid model. The ring current effect on the Earth was calculated from AMPTE/CCE measurements. In accordance with (Alexeev et al., 1996; Dremukhina et al., 1999) the calculated values of magnetic fields of various sources of the magnetospheric field at the Earth's surface were multiplied by a factor of 1.5 in order to take into account the effect of induced currents in the perfectly conducted Earth (Dessler and Parker, 1959).

3. Discussion

Calculation of the magnetospheric magnetic field variations on the Earth's surface are presented in Fig. 3. The calculated magnetic fields of currents on the magnetopause, B_{CF}, of the tail current system, B_T, and of the ring current, B_R, are approximately of the same order of magnitude (see Fig. 3a). Fig. 3b shows a rather good agreement of model calculations of $B_M = B_R + B_T + B_{CF}$ with Dst (heavy solid line). It attracts attention that all compounds of the calculated summary variation of the magnetic field give significant and comparable contribution to Dst. During disturbances associated with substorm activity the influence of the magnetotail current system increases, and the total contribution of the ring and tail currents can significantly exceed the observed Dst value. These excesses are compensated by the opposite-sign effect of the currents on the magnetopause. The increasing solar wind dynamical pressure leads to a decrease of a distance to the subsolar point. The magnetic field of the magnetopause currents measured on the Earth's surface is inversely proportional to a cubed change of R_1 (Mead, 1964). Such strong dependence of the magnetic fields on the magnetopause on R_1 leads to an increase of the magnetic field on the magnetopause by a factor of 3 with R_1 changing from $10R_E$ to $7R_E$. Here the B_{CF}-value on the Earth's surface can change from 30 to 90 nT (taking into account the induced terrestrial currents).

The current systems discussed above are influenced by processes in the interplanetary medium as well as in the magnetosphere. Changes of the magnetic fields depend on the parameters most strongly affecting the current systems. For the ring current this parameter is the injection intensity which determines the total energy of ring current particles. For currents on the magnetopause, the most significant parameter is the solar wind pressure, while for the tail current system there are the solar wind pressure and the magnetic flux in the magnetotail lobe, Φ_∞. These parameters define the time scales of the above noted current systems and reveal themselves in variations of the Dst profile. A smooth change of the profile corresponds to the development and decay of the ring current with the characteristic time of tens of hours. More rapid changes of the Dst profile correspond to enhancements of magnetic flux in the magnetotail lobes associated with the development of a substorm. These results confirm those obtained by Alexeev et al. (1996). It should be emphasized that all terms comprising B_M give significant and comparable contribution to Dst, including the magnetopause current contribution B_{CF}, which was not investigated in Alexeev et al. (1996).

Fig. 4 represents the comparison of the measured and calculated magnetic fields along the GOES-6 orbit during the magnetic storm on 23–27 November 1986. We can see (Fig. 4a) that the modelled magnetic field (dashed line) describes the measurements (solid line) well. The average discrepancy is about 15%. There exists the regular difference

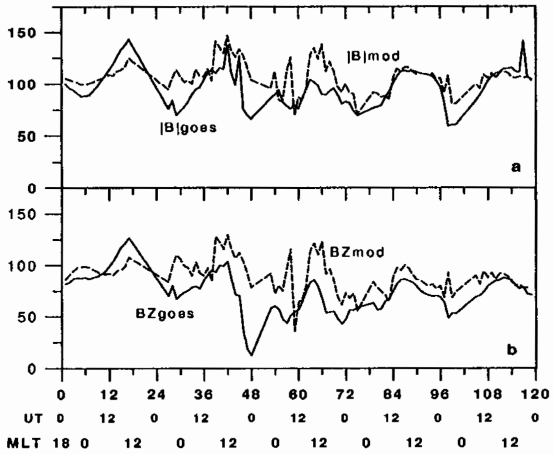

Fig. 4. The comparison of measured (solid line) and calculated (dashed line) magnetic fields along the GOES-6 orbit module (a) and B_z GSM (b) during the magnetic storm on 23–27 November 1986.

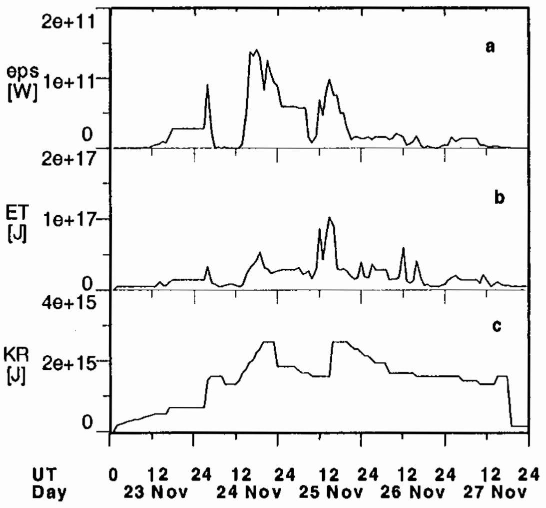

Fig. 5. The energy input rate through the magnetopause (W) (a), the magnetic energy stored in the geomagnetic tail (J) (b) and the kinetic energy of ring current particles (J) (c), in the course of the magnetic storm on 23–27 November 1986.

in B_z component: the calculated magnetic field is as a rule larger than the measured one (see Fig. 4b). We can see that the ring current is not underestimated in our calculations: its increase will cause the more significant discrepancy, since the ring current magnetic field is northward in this region. Such a regular difference also cannot be explained by region 1 field aligned currents whose contribution must have an azimuthal asymmetry and is rather connected with the geotail or magnetopause currents.

Fig. 5 represents the hourly averaged total energy input rate in the magnetosphere (Fig. 5a) calculated in terms of the

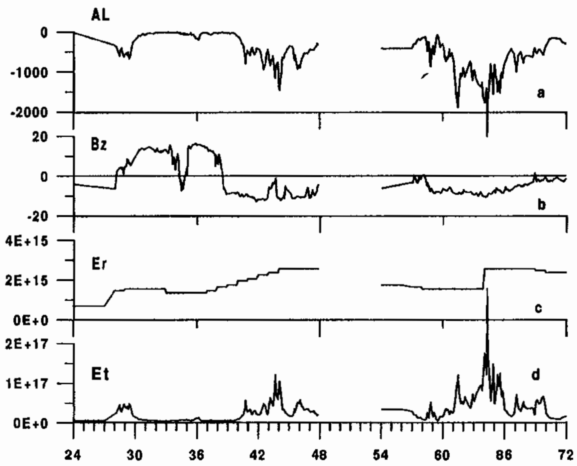

Fig. 6. AL index (nT) (a), B_z IMF (nT) (b), the kinetic energy of ring current particles (J) (c), and the magnetic energy stored in the geomagnetic tail (J) (d), during 24 and 25 November 1986 (5 min averaged data).

Akasofu coupling function (Perreault and Akasofu, 1978):

$$\varepsilon = |E||B|(l_0 \sin^2(\theta/2))^2/4\pi$$

and the magnetic energy stored in the magnetotail (Fig. 5b) calculated in terms of the paraboloid model (see Alexeev et al., 1996):

$$E_t(t) = \Phi_\infty I_t$$

(here $l_0 = 7R_E$, θ is an angle between the IMF and the magnetospheric magnetic field near the magnetopause subsolar point, and I_t is the total magnetospheric tail current). We can see that the energy stored in the magnetotail correlates strongly with the energy flow in the magnetosphere generated by the solar wind–magnetosphere dynamo. The total kinetic energy of ring current particles (Fig. 5c) calculated from AMPTE/CCE data is much smaller than energy stored in the magnetotail. However, because of its proximity and location ring current particles produce the part of Dst variation comparable with geotail, as was discussed above. The ring current evolution consists of several periods of development and decay. We can see in Fig. 5 the three ring current intensifications on approximately 03:00 24 November, 14:00 24 November, and 16:00 25 November apparently associated with particle injections from tail current. Let us consider the small scale structure of these events.

Fig. 6 represents 5 min averaged AL index (Fig. 6a); B_z IMF (nT) (Fig. 6b); the kinetic energy of ring current particles (Fig. 6c); and the magnetic energy stored in the geomagnetic tail (Fig. 6d) in the period from 00:00 UT 24 November till 24:00 25 November 1986 when all the three ring current intensifications took place.

We can see that ring current energy growth takes place when B_z IMF is negative. This growth stopped as a rule when IMF turns northward (see the first two ring current intensifications) or when negative B_z become larger. We can also see that periods of ring current energy increase corresponding to the periods of high auroral activity indicated by AL index. On the other hand, the ring current energy increase stops when AL approaches the most significant values. It confirms in general the main conclusion of Iyemory and Rao (1998), that Dst does not show any development after substorm onset. However, in our case we can see no single substorm but rather a series of substorms or substorm-related phenomena.

Fig. 6 represents the magnetic storm dynamics on substorm-related time scales. It demonstrates the ambivalent role of substorms in the ring current dynamics. We can see as a rule, several substorms during each period of ring current enhancement. During substorm growth phases, particle injection from the geotail carries the ring current. We can suggest that when geotail enhanced currents are moving to the Earth, particle injection into the ring current and the total energy of the ring current particles are increased. On the other hand, during substorm expansion phases, we can see phenomena such as substorm dipolarization, substorm current wedge formation and the following near-Earth tail current decay. In Fok et al. (1999) the total H^+ energy growth in the $R > 6.6R_E$ region during substorm expansion phase was explained by substorm dipolarization. Moreover, just after substorm current wedge formation, when the magnetospheric tail is closest to the Earth, part of the energy earlier transported into ring current also goes to the ionosphere (Iyemory and Rao, 1996) and ring current development slows down (Alexeev, 1996). After a series of substorms, when magnetospheric tail is moving earthward and back, most of the geotail energy is dissipated at the ionospheric level and ring current growth slows down or even stops.

4. Conclusion

Ground-based- and satellite-data were used to study the dynamics of magnetospheric current systems in the course of the magnetic storm on 23–27 November 1986. The ring current magnetic field is calculated at the Earth's surface, using measurements obtained onboard the AMPTE/CCE spacecraft. Magnetic fields of the magnetotail currents and magnetopause currents are calculated in terms of the paraboloid magnetospheric model, using measurements onboard the IMP-8, DMSP-F6, DMSP-F7 spacecrafts and those at auroral magnetic observatories (AL index). The summary field calculated on the Earth's surface was compared with Dst variations calculated using the measurements at low-latitude observatories.

Calculations show that the Dst variation is connected not only with the ring current but also with other sources of the magnetospheric magnetic field, in particular, the magnetotail currents and the currents on the magnetopause are responsible for a considerable fraction of the disturbance. The structure and intensity of Dst variation are defined by interaction of all sources of the magnetospheric magnetic field, affecting the joint profile of the disturbance. The energy stored in the geomagnetic tail strongly correlates with the energy flow in the magnetosphere generated during solar wind–magnetosphere coupling. The energy stored in the ring current increases after B_z IMF-southward turning. The ring current energy growth slows down and even stops during periods of high auroral activities when the part of the energy stored in the magnetospheric tail is spent at the ionospheric level.

Acknowledgements

The authors gratefully acknowledge the assistance M. Greenspan in providing data of ring current particle energy for the magnetic storm under consideration. The authors thank Drs. H. Singer, D. Wilkinson and G. Ushomirskiy (National Geophysical Data Center/NOAA) for the GOES-6 data. The authors would like to acknowledge both referees for the careful reading of the manuscript and for the useful comments and corrections. The investigation was supported by Russian Foundation for Basic Research Grant 98-05-64784.

References

Alexeev, I.I., 1978. Regular magnetic field in the Earth's magnetosphere. Geomagnetizm i Aeronomia 18, 656–665 (in Russian).

Alexeev, I.I., 1996. Magnetospheric key parameters and energy transfer during substorm. Proceedings of the Third International Conference on Substorms (ICS-3). Versailles, France, 12–17 May 1996; ESA SP-389, 651–654.

Alexeev, I.I., Belenkaya, E.S., Kalegaev, V.V., Feldstein, Ya.I., Grafe, A., 1996. Magnetic storms and magnetotail currents. Journal of Geophysical Research 101, 7737–7747.

Alexeev, I.I., Kalegaev, V.V., Feldstein, Ya.I., 1992. Modelling of magnetic field in strongly disturbed magnetosphere. Geomagnetizm i Aeronomia 32, 8–14 (in Russian).

Arykov, I.I., Maltsev, Yu.P., 1993. Contribution of various sources to geomagnetic storm field. Geomagnetizm i Aeronomia 33, 67–74 (in Russian).

Campbell, W.H., 1973. The field levels near midnight at low and equatorial geomagnetic stations. Journal of Atmospheric and Terrestrial Physics 35, 1127–1146.

Dessler, A.J., Parker, E.N., 1959. Hydromagnetic theory of geomagnetic storms. Journal of Geophysical Research 64, 2239–2252.

Dremukhina, L.A., Feldstein, Ya.I., Alexeev, I.I., Kalegaev, V.V., Greenspan, M., 1999. Structure of the magnetospheric magnetic field during magnetic storms. Journal of Geophysical Research 104, 28,351–28,360.

Iyemory, T., Rao, D.R.K., 1996. Decay of the Dst field of geomagnetic disturbance after substorm onset and its implication to storm–substorm relation. Annales de Geophysique 14, 608–618.

Fok, M.C., Moore, T.E., Delcourt, D.C., 1999. Modelling of inner plasma sheet and ring current during substorms. Journal of Geophysical Research 104, 14,557–14,570.

Friedrich, E., Rostoker, G., Connors, M.G., McPherron, R.L., 1999. Influence of the substorm current wedge on the Dst index. Journal of Geophysical Research 104, 4567–4576.

Greenspan, M.E., Hamilton, D.C., 2000. A test of the Dessler–Parker–Sckopke relation during magnetic storms. Journal of Geophysical Research 105, 5419–5430.

Ho, C.M., Tsurutani, B.T., 1997. Distant tail behavior during high speed solar wind streams and magnetic storms. Journal of Geophysical Research 102, 14,165–14,175.

Kalegaev, V.V., Alexeev, I.I., Feldstein, Y.I., Gromova, L.I., Grafe, A., Greenspan, M., 1998. Tail lobe magnetic flux and dynamics of the Dst disturbance in the course of magnetic storms. Geomagnetism i Aeronomia 38, 10–16 (in Russian).

Kalegaev, V.V., Lyutov, Yu.G., 2000. The solar wind control of the magnetopause. Advances in Space Research 25, 1489–1492.

Kaufmann, T.G., 1987. Substorm currents: growth phase and onset. Journal of Geophysical Research 92, 7471–7480.

Kokubun, S., Frank, L.A., Hayashi, K., Kamide, Y., Lepping, R.P., Mukai, T., Nakamura, R., Paterson, W.R., Yamamoto, T., Yumoto, K., 1996. Large field events in the distant magnetotail during magnetic storms. Journal of Geomagetism and Geoelectricity 48, 561–576.

Lopez, R.E., von Rosenvinge, T., 1993. A statistical relationship between the geosynchronous magnetic field and substorm electrojet magnitude. Journal of Geophysical Research 98, 3851–3857.

Mead, G.D., 1964. Deformation of the geomagnetic field by the solar wind. Journal of Geophysical Research 69, 1181–1195.

Perreault, P., Akasofu, S.-I., 1978. A study of geomagnetic storms. Geophysical Journal of the Royal Astronomical Society 54, 547–573.

Pulkkinen, T.I., Baker, D.N., Pellinen, R.J., Buchner, J., Koskinen, H.E.J., Lopez, R.E., Dyson, R.L., Frank, L.A., 1992. Particle scattering and current sheet stability in the geomagnetic tail during the substorm grows phase. Journal of Geophysical Research 97, 19,283–19,297.

Sckopke, N., 1966. A general relation between the energy of trapped particles and the disturbance field near the Earth. Journal of Geophysical Research 71, 3125–3130.

Sibeck, D.G., Lopez, R.E., Roelof, E.C., 1991. Solar wind control of the magnetopause shape, location, and motion. Journal of Geophysical Research 96, 5489–5495.

Turner, N.E., Baker, D.N., Pulkkinen, T.I., McPherron, R.L., 2000. Evaluation of the tail current contribution to Dst. Journal of Geophysical Research 105, 5431–5440.